Optical properties of tropospheric aerosols determined by lidar and spectrophotometric measurements (Photochemical Activity and Solar Ultraviolet Radiation campaign)

Franco Marenco, Vincenzo Santacesaria, Alkiviadis F. Bais, Dimitris Balis, Alcide di Sarra, Alexandros Papayannis, and Christos Zerefos

We present the results of the aerosol measurements carried out over the Aegean Sea during the Photochemical Activity and Solar Ultraviolet Radiation campaign held in Greece during June 1996. Simultaneous observations performed with a lidar and a double-monochromator spectrophotometer allowed us to retrieve the optical depth, the Ångström coefficient, and the backscatter-to-extinction ratio. The Sun photometric data can be used to improve quantitative aerosol measurements by lidar in the Planetary Boundary Layer. Systematic errors could arise otherwise, because the value of the backscatter-to-extinction ratio has to be supplied. Instead this ratio can be retrieved experimentally by use of an iterative solution of the lidar equation. © 1997 Optical Society of America

Key words: Aerosols, optical depth, backscatter-to-extinction ratio, Ångström coefficient, lidar signal inversion.

1. Introduction

Particulate matter (aerosol) in the atmosphere has been extensively studied by means of the elastic backscattering lidar.[1–3] Despite the high vertical and temporal resolution, attempts to obtain quantitative information from these measurements can lead to large inaccuracies because assumptions about the atmospheric target itself are necessary for the inversion of the signal. This is valid for measurements both in the stratosphere and in the troposphere, but for the case of stratospheric aerosol the properties of the particles are generally well known. They are believed to be composed of sulfuric acid and water, whose weight fractions depend on humidity and temperature[4]; furthermore, their size distribution can be assumed to be more or less constant, at least in nonvolcanic periods. (It should be mentioned, though, that recent studies seem to indicate that the composition of the stratospheric particles is still uncertain.[5])

The tropopause is characterized by low aerosol content (see, e.g., Ref. 6), and the middle stratosphere is devoid of particles: this results in two aerosol-free regions, one above and one below the stratospheric aerosol layer. This circumstance facilitates lidar signal inversion and allows good retrieval of the range-resolved aerosol backscattering and extinction coefficients, even though some distortion of the profiles cannot be avoided.[7] The distortion is intrinsic in the assumption that the aerosol backscatter-to-extinction ratio is constant with height. The aerosol-free regions above and below the aerosol layer can be used as boundary conditions for the lidar inversion. In this way the mean value of the backscatter-to-extinction ratio of the aerosol layer can be inferred, together with the backscattering and

When this research was performed, F. Marenco, V. Santacesaria, A. F. Bais, D. Balis, A. Papayannis, and C. Zerefos were with the Laboratory of Atmospheric Physics, Aristotle University of Thessaloniki, Thessaloniki 54006, Greece. F. Marenco is now with the European Space Research and Technology Centre, Earth Sciences Division, Noordwijk, The Netherlands. V. Santacesaria is now with the Istituto di Ricerca sulle Onde Elettromagnetiche Nello Carrara, Firenze, Italy. A. di Sarra is with the Department of Physics, University La Sapienza, Rome, Italy, and Ente per le Nuove Tecnologie, l'Energia e l'Ambiente, S. Maria di Galeria, Italy. A. Papayannis is also with the Laser and Applications Laboratory, National Technical University of Athens, Athens, Greece.

Received 4 November 1996; revised manuscript received 21 March 1997.

0003-6935/97/276875-12$10.00/0

extinction coefficient profiles.[8] This same scheme may be used in the case of thin tropospheric clouds.

In the study of lower tropospheric particulate matter, no clean layer can be assumed below the aerosols, since their highest concentration is to be found near the ground. In this case the approach proposed by Fernald[9] and Klett[10] is often used to invert the lidar signal profile, and the aerosol backscatter-to-extinction ratio has to be given an *a priori* value; this assumption severely limits the possibility of quantitatively measuring the optical parameters of the aerosols. Therefore Planetary Boundary Layer (PBL) probing by lidar has often been limited to qualitative descriptions of the aerosol behavior. With the aerosols used as tracers of the atmospheric dynamics, parameters of the PBL such as mixed-layer depth, entrainment zone boundaries, convective cell structure, etc., have been determined, providing useful information for the study of atmospheric transport processes and other inferences of air motion.[11–14]

Takamura *et al.*[15] showed that the uncertainty in the backscatter-to-extinction ratio can be removed by using supplementary information from a Sun photometer. Quantitative measurements of aerosols and their spatial distribution are of considerable importance in atmospheric physics and are essential for estimating the effects of aerosols on climate. These effects are direct (diffusion and attenuation of the solar radiation penetrating the atmosphere) and indirect, as, for instance, through the enhancement of cloud formation.

At the Laboratory of Atmospheric Physics of the Aristotle University of Thessaloniki attempts have been made to study the influence of lower tropospheric aerosols on global radiation reaching the ground in the UV spectral range.[16,17] Radiation spectra obtained with the ultraviolet spectrophotometer of the Laboratory of Atmospheric Physics were combined with lidar-derived aerosol measurements, and a radiation transfer model was used to validate the results obtained. To allow us to model the radiation field the absolute optical properties of the aerosols are needed. As stated above, this information is not obtainable from the lidar signal, unless strong assumptions are made or complementary observations are available.

In this paper we present a comparison of aerosol observations obtained at the same wavelength with two different techniques during the Photochemical Activity and Solar Ultraviolet Radiation (PAUR) campaign held in Greece during June 1996. Aerosol characteristics have been derived by lidar, whose signals have been analyzed by the Fernald–Klett method, and by direct-Sun photometric measurements. With the latter having been taken spectrally, the wavelength dependence of the aerosol optical depth in the UV spectral range has also been retrieved. Finally, we suggest a method that enables one to combine these two types of measurements to obtain absolute and range-resolved aerosol backscattering and extinction coefficients. This allowed us to deduce the backscatter-to-extinction ratio experimentally.

2. Inversion of the Lidar Signal

A. General Remarks

Under the hypothesis of single scattering, for the case of a monostatic and vertically looking lidar, the detected signal $N(z)$ as a function of the altitude z is given by the following formula, known as the lidar equation[18]:

$$N(z) = K_L \frac{\beta_R(z) + \beta_P(z)}{(z - z_L)^2} \times \exp\left\{-2 \int_{z_L}^{z} [\alpha_R(z) + \alpha_P(z)]\mathrm{d}z\right\}, \quad (1)$$

where $\beta_R(z)$ and $\beta_P(z)$ are the backscattering coefficients for the molecular (Rayleigh) and particulate (Mie) components of the atmosphere, respectively; $\alpha_R(z)$ and $\alpha_P(z)$ are the extinction coefficients for these two components; and z_L is the altitude of the lidar system. In the extinction coefficients, $\alpha_R(z)$ and $\alpha_P(z)$, effects of both scattering and absorption are included. K_L is known as the lidar constant, and it depends on several instrumental parameters, such as laser output, receiver aperture, and the efficiency of the optics and of the quantum detectors. Equation (1) is valid provided that the background level that is due to skylight and detector dark current has been duly subtracted. In what follows we assume that $\beta_R(z)$ and $\alpha_R(z)$ are known functions of height. These quantities can be obtained by an independent measurement carried out with balloon-borne detectors or by use of a suitable atmospheric model (such as the U.S. Standard Atmosphere[19]).

To retrieve the aerosol parameters from the measured signal we still have two unknowns, $\beta_P(z)$ and $\alpha_P(z)$, with only one equation. In order to remove this indeterminacy a relationship between the aerosol backscattering and extinction coefficients has to be assumed. Unless more information is available, it is often assumed that the particulate backscatter-to-extinction ratio is constant with height:

$$\beta_P(z)/\alpha_P(z) = C. \quad (2)$$

This ratio depends on several factors, such as chemical composition, shape, and size distribution of the aerosol particles. The atmosphere being layered, the temperature and humidity fields present vertical inhomogeneity, and this influences the properties of the aerosols in equilibrium with the gases of the molecular atmosphere. It is therefore reasonable to expect a height dependence of the ratio C. It therefore has to be stressed that assumption (2) is made because there are no other practical possibilities for inverting the lidar equation.

Two boundary conditions are necessary to allow us to assign values to the constants K_L and C. Boundary conditions can be set, for instance, at regions

assumed to be aerosol free, where the particulate backscattering coefficient can be set equal to zero. In principle K_L could be known (absolutely calibrated lidar). However, it is often preferable not to perform an absolute calibration, since the experimental parameters that determine K_L may fluctuate (e.g., the laser output power). In that case the lidar return is calibrated *a posteriori* by the choice of an aerosol-free region in which the data are fitted to a molecular profile (a lidar signal profile calculated taking into account only molecular backscattering.)

B. Fernald–Klett Solution of the Lidar Equation

Fernald[9] and Klett[10] gave an analytical solution to Eqs. (1) and (2). The boundary conditions needed are the following:

(i) The backscatter-to-extinction ratio as known from an appropriate model or an independent measurement. If known, even a ratio that is variable with height may be used. In published models values for tropospheric aerosols can be found ranging between 0.01 and 0.05 according to the type of air mass (rural, urban, or maritime); see, e.g., Refs. 15 and 20–22.

(ii) The atmospheric backscattering coefficient $\beta_m = \beta_R(z_m) + \beta_P(z_m)$ at a far-end reference height z_m. Generally, an aerosol-free region where the signal follows the molecular profile well can be found in the lidar return, and β_m is assumed equal to $\beta_R(z_m)$.

The assumption that C is known *a priori* is probably the largest source of systematic error within this lidar inversion scheme. The choice of the type of air mass (rural, urban, or maritime) can be problematic, since the backward trajectories of the studied air masses for a few days before the measurement should be known. Moreover, the values of C reported in the literature for each model are climatological averages or the result of calculations carried out for some standard cases. Thus it is expected that large discrepancies exist. Kovalev[23] shows that the resulting error is larger when the vertical gradient of the aerosol extinction coefficient is large, which is usually the case for the lower troposphere.

C. A Different Approach: Combination of Photometric and Lidar Data

Kovalev[24] has considered the possibility of using the optical thickness of an aerosol layer as a boundary condition for the inversion of the lidar equation. In his approach a constant or range-dependent value of C still has to be given *a priori*, but it is no longer necessary to know the atmospheric backscattering coefficient β_m at a reference height z_m. Takamura *et al.*[15] considered instead the possibility of removing the indeterminacy in the backscatter-to-extinction ratio by combining lidar data with independent measurements of the optical depth τ. In their method the Fernald–Klett analysis is performed with a few different values of C, and then interpolation in the (C, τ) plane is performed to determine the correct value.

We describe here an alternative inversion method, which through an iterative procedure allows one to determine the aerosol backscattering and extinction coefficients by using as boundary conditions (i) the optical depth τ^* of the aerosols in the considered altitude range (z_0, z_m) and (ii), as in the Fernald–Klett approach, the total backscattering coefficient β_m (due to molecules and aerosols) at a far-end reference height z_m. We stress that the assumption that C is constant with height is still necessary, but this value can now be determined through the retrieval procedure. This method was first used by the researchers of the University of Rome for the study of the Pinatubo aerosol layer in the lower stratosphere.[8] The version that we present here has been slightly adapted for the study of lower tropospheric aerosol. In the original version of this algorithm, applied to stratospheric aerosols, two clean regions above and below the aerosol layer were assumed. Then τ^* could be deduced from the lidar signal itself, by examination of the attenuation of the molecular profile through the aerosol layer. In the case that no clean layer is present below and that the lidar is not absolutely calibrated, τ^* must be taken from an independent source.

The lidar equation (1) is solved by direct substitution by successive iterations. We restate this equation by conglobating the transmissivity factor for the (z_L, z_0) range into the constant K_L, thus obtaining a new constant K_L^*:

$$N(z) = K_L^* \frac{\beta_R(z) + \beta_P(z)}{(z - z_L)^2} \times \exp\left\{-2 \int_{z_0}^{z} [\alpha_R(z) + \alpha_P(z)]\mathrm{d}z\right\}. \quad (3)$$

The procedure is based on the comparison of $N(z)$ with a molecular profile, i.e., a profile calculated with the above formula, with $\beta_P(z) = 0$ (but still taking into account aerosol extinction):

$$M(z) = K_L^* \frac{\beta_R(z)}{(z - z_L)^2} \times \exp\left\{-2 \int_{z_0}^{z} [\alpha_R(z) + \alpha_P(z)]\mathrm{d}z\right\}. \quad (4)$$

K_L^* is determined by using the boundary conditions and solving the following equation (signal normalization):

$$N(z_m) = K_L^* \frac{\beta_m}{(z_m - z_L)^2} \times \exp\left[-2 \int_{z_0}^{z_m} \alpha_R(z)\mathrm{d}z - 2\tau^*\right]. \quad (5)$$

As a first approximation the aerosol extinction coefficient is assumed to be independent of height:

$$\alpha_P'(z) = \alpha_P' = \frac{\tau^*}{z_m - z_0}, \tag{6}$$

and by substitution into Eq. (4) an approximate molecular profile $M'(z)$ is calculated. The first approximation of the particulate backscattering coefficient is obtained from the ratio of Eqs. (3) and (4),

$$\beta_P'(z) = \beta_R(z)\left[\frac{N(z)}{M'(z)} - 1\right], \tag{7}$$

and by integration an estimate of the aerosol integrated backscattering is computed:

$$I_P' = \int_{z_0}^{z_m} \beta_P'(z)\mathrm{d}z. \tag{8}$$

The first estimate of the aerosol backscatter-to-extinction ratio is then obtained from the ratio of the integrated backscattering and the optical depth:

$$C' = I_P'/\tau^*. \tag{9}$$

This value of C' allows us to find a second estimate of the extinction coefficient:

$$\alpha_P''(z) = \beta_P'(z)/C'. \tag{10}$$

Equations (4) and (7)–(10) are then reiterated by use of $\alpha_P''(z)$ to derive a new molecular profile $M''(z)$; this yields new values for the backscattering coefficient $\beta_P''(z)$, the integrated backscattering I_P'', and the backscatter-to-extinction ratio C''. The procedure is repeated until

$$\left|\frac{C^{(n)} - C^{(n-1)}}{C^{(n-1)}}\right| < \varepsilon. \tag{11}$$

Very few iterations have been found to be necessary for the results to converge to a stable solution (typically less than six for $\varepsilon = 0.0005$), and an excellent agreement with the Fernald–Klett analytic method is obtained when the retrieved value of C is used.

3. Experimental Setup

An elastic backscattering lidar and a Brewer spectrophotometer were operated on a continuous basis in daytime during the PAUR experiment. One of the experiment sites was the Greek island Agios Efstratios (39.5 °N, 25 °E), and the period of measurement lasted between 3 and 14 June 1996. This island is in the Aegean Sea, far from cities, industries, and other major pollution sources, at a distance of ~30 km from the island Limnos, ~110 km from mainland Greece, and ~80 km from mainland Turkey. The lidar was placed at sea level, while the Brewer was located at an altitude of ~50 m. A brief description of the instruments is given in the following paragraphs.

A. Lidar

The mobile lidar system of the Laboratory of Atmospheric Physics operates at the wavelengths 355 and 532 nm.[25] The complete overlap of the laser beam with the telescope field of view is at a range of ~500 m as estimated by geometrical form factor calculations performed according to the procedures of Halldorsson and Langerholc.[26] The data are recorded on a continuous basis, with a verical resolution of 15 m and a temporal resolution of 10 min. In the lidar inversion the reference height has been chosen, for each profile, in a region where the signal followed the molecular profile, generally between 5 and 6 km. The reference value has been chosen as $\beta_m = \beta_R(z_m)$. The backscatter-to-extinction ratio assumed for the Fernald–Klett inversion was always $C = 0.05$, a value representative of maritime aerosols.[20]

B. Brewer Spectrophotometer

The spectra of both the direct and the global solar ultraviolet irradiance at the ground were measured with a double-monochromator Brewer spectrophotometer as described by Bais *et al.*[27] These spectra cover the spectral range from 285 to 366 nm, in steps of 0.5 nm and with a resolution of 0.64 nm (FWHM); their absolute calibration is maintained regularly by use of a 1000-W quartz-halogen standard source of spectral irradiance, traceable to National Institute of Standards and Technology standards. In particular, the absolute calibration of the direct irradiance spectra followed the procedure described by Bais.[28] In the field a set of two 50-W lamps was used to monitor the instrument stability and to detect any changes in its absolute calibration. On the basis of these measurements no detectable change was found during the campaign after the time of the last absolute calibration.

The Brewer spectrophotometer was programmed to perform a series of global and direct-Sun scans every 30 min from sunrise to sunset. Each of these scans lasted ~10 min, so the remaining time was devoted to a wavelength alignment calibration, followed by a measurement of the total-column ozone.

4. Aerosol Optical Depth from Spectrophotometric Measurements

The total-column optical depth of the aerosols in the UV region, as well as its spectral dependence and time variations, can be retrieved from the direct-Sun irradiance measured at ground level. The common assumption made is that the atmosphere is plane parallel. Owing to the curvature of the Earth, the optical path is actually longer than it would be for a plane-parallel atmosphere. This can lead to a systematic error (overestimate of the optical depth). However, this error is small compared with other sources of error for solar zenith angles $\theta \leq 75°$. All data corresponding to larger solar zenith angles have

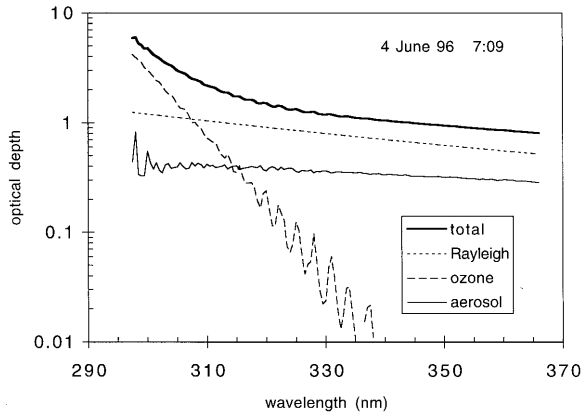

Fig. 1. Total optical depth of the atmosphere as a function of wavelength, measured by the Brewer spectrophotometer. Also shown are the contributions from Rayleigh scattering, ozone, and aerosols. For this measurement the solar zenith angle was 66° and the columnar amount of ozone was 312 D.U.

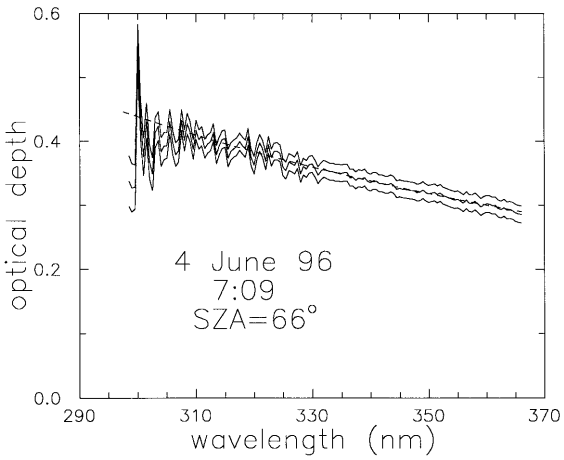

Fig. 2. Center solid curve: aerosol optical depth as a function of wavelength. The dashed curve represents a least squares fit with a λ^{-m} dependence. The other solid curves show the amplitude of the experimental error ($\pm\Delta\tau_P$).

been discarded, and the optical depth has been derived from the following equation:

$$\tau_P(z_B, \infty, \lambda) = (\cos\theta) \ln \frac{I_0(\lambda)}{I(\lambda)} - \frac{p}{p_0}\tau_R(\lambda) - D_{O_3}k_{O_3}(\lambda)\frac{\ln 10}{1000}, \quad (12)$$

where

- z_B is the altitude of the Brewer spectrophotometer,
- λ is the wavelength,
- θ is the solar zenith angle,
- $I(\lambda)$ is the measured irradiance,
- $I_0(\lambda)$ is the solar extra-terrestrial irradiance,
- p is the atmospheric pressure at height z_B,
- p_0 is the standard atmospheric pressure (1013.25 mbar),
- $\tau_R(\lambda)$ is the optical depth due to Rayleigh scattering from sea level to infinity under standard pressure condition,
- D_{O_3} is the ozone column in Dobson units (D.U.) measured with the Brewer spectrophotometer,
- $k_{O_3}(\lambda)$ is the absorption coefficient of O_3 in inverse centimeters (cm^{-1}).

Figure 1 shows the contribution of the different terms in Eq. (12) as a function of wavelength.

The extraterrestrial spectrum $I_0(\lambda)$ was measured with the same Brewer spectrophotometer by the Langley extrapolation method in July 1995.[28] The measurement was carried out at the Izana Observatory, Tenerife, situated at an altitude of 2370 m in an aerosol-free and stable ozone condition. The resulting spectrum is generally in good agreement with the measurements of the satellite-borne Solar Ultraviolet Spectral Irradiance Monitor experiment.[29] A spectrum obtained with the same spectrophotometer is adopted here to minimize the error in the absolute calibration and the inaccuracy resulting from the use of data obtained with a different slit function. The solar spectrum was also corrected to account for the seasonal variation of the Sun–Earth distance.

The Rayleigh optical depth was calculated according to Hansen and Travis[30]:

$$\tau_R(\lambda) = 0.09364\left(\frac{\lambda}{\lambda_0}\right)^{-4}\left[1 + 0.0374\left(\frac{\lambda}{\lambda_0}\right)^{-2} + 0.00142\left(\frac{\lambda}{\lambda_0}\right)^{-4}\right], \quad (13)$$

where $\lambda_0 = 550$ nm. A comprehensive survey of the different fitting equations that can be used to compute Rayleigh optical depths can be found in the article by Teillet.[31]. The formula given above best matches the result of his exact calculations performed for standard atmospheric conditions.

The ozone absorption cross sections that we used are those measured by Molina and Molina[32] for the 285–350-nm range, extended up to 355 nm with the values obtained by Cacciani *et al.*[33] No values were available for $\lambda > 355$ nm, and the ozone term has been neglected at those wavelengths.

The experimental error in the aerosol optical depth obtained with Eq. (12) can be estimated as follows:

$$(\Delta\tau_P)^2 = (\cos^2\theta)\left[\left(\frac{\Delta I_0}{I_0}\right)^2 + \left(\frac{\Delta I}{I}\right)^2\right] + \left(\frac{\Delta D_{O_3}}{D_{O_3}}\tau_{O_3}\right)^2, \quad (14)$$

where τ_{O_3} is the contribution that is due to ozone absorption, given by the last term in Eq. (12). All errors are statistical (1σ), and the errors in the Rayleigh term and the ozone absorption coefficients have been neglected.

The aerosol optical depth is expected to be a smooth function of wavelength, but as can be seen in Fig. 2,

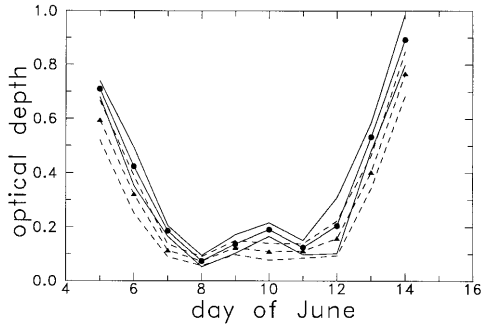

Fig. 3. Mean daily values of optical depth as derived (solid curve with filled circles) by the Brewer spectrophotometer and (dashed curve with triangles) by lidar with the Fernald–Klett method. The solid and dashed curves without circles or triangles show the corresponding ±1 standard deviation, which is a measure of the variability of the measured quantity during the day.

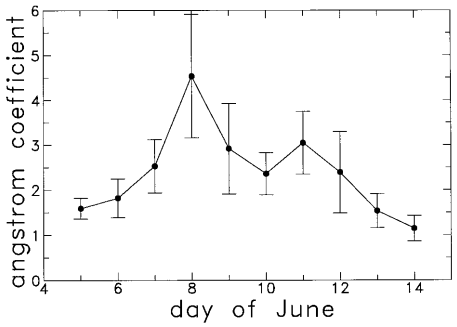

Fig. 4. Mean daily values of the Ångström coefficient, as derived by Brewer observations. The error bars show ±1 standard deviation.

small fluctuations are present, especially for $\lambda < 330$ nm. This is believed to be caused mostly by an imperfect removal of the ozone contribution, since the absorption coefficients present an oscillatory behavior and, moreover, are temperature dependent. It has to be pointed out that absorption by sulfur dioxide, which has not been taken into account, may contribute to these fluctuations as well. To remove them, a power-law dependence on wavelength has been assumed[34]:

$$\tau_P(\lambda) = \tau_0(\lambda/\lambda_0)^{-m}, \tag{15}$$

where m is known as the Ångström coefficient or Ångström exponent and λ_0 is a chosen wavelength. The constants τ_0 and m have been determined for each direct-Sun scan by a least-squares fit of the optical depth data between 320 and 355 nm: the data below 320 nm are believed to be affected by high measurement errors owing to the low intensity of the sunlight reaching the ground (high ozone absorption); the data above 355 nm have been discarded owing to the nonavailability of O_3 cross sections.

5. Results

In this section we present the results of the aerosol measurements obtained during the first two weeks of June 1996 on Agios Efstratios. The weather conditions were excellent throughout the campaign, and only in very few cases did clouds affect the measurements. The cloudy data have been removed from the data set. The general results are given here, mainly with the aim of comparing the two measurement techniques and showing the ability of both to highlight the evolution of short-term features. The diurnal evolution of the aerosol, in relation to the meteorological conditions, will be the object of a separate study.

A. Lidar and Brewer Measurements of Optical Depth Analyzed Separately

In Fig. 3 we show the daily mean values of the optical depth τ_B at 355 nm obtained with the Brewer spectrophotometer for the altitude range from 50 m to infinity (outer space). Also shown are the daily means of the aerosol optical depth derived by lidar at the same wavelength for the 0.6–5-km range, τ_L, deduced with the Fernald–Klett method and vertical integration of the extinction coefficient. The average values throughout the campaign are $\tau_B = 0.35$ and $\tau_L = 0.28$ (with standard deviations 0.28 and 0.24, respectively). As can be seen the aerosol load showed a large variability: high values of τ_B (larger than 0.4) were observed until 6 June, with a value as large as 0.7 on 5 June. A period of very low values followed between 7 and 12 June ($\tau_B < 0.2$). Finally, the optical depths showed a strong increase on 13 and 14 June, reaching a daily mean value of 0.9. The lidar-derived optical depths show good agreement with the Brewer data. They are generally smaller, as is expected, since the altitude range scanned by lidar does not cover the total column.

The wavelength dependence of the optical depth, also resulting from the Brewer measurements, can be summarized by the Ångström coefficient m given by Eq. (15). In Fig. 4 the daily means of m are depicted as a function of time. The average Ångström coefficient was 2.4, but high variability was observed (standard deviation 1). Lower values, approximately 1.5–2, were found on high-turbidity days ($0.3 \leq \tau_B \leq 0.9$), and values of approximately 2.5–3 were observed on low-turbidity days ($\tau_B \leq 0.2$). The two extremes were on 14 June, with $m \sim 1$, and on 8 June, with $m \sim 4$. It has to be noted that these two days are also those in which respectively the highest and the lowest turbidity were reached.

The optical depths derived from the Brewer spectrophotometer and the lidar observations are shown in Fig. 5 as a function of local time for the whole campaign period at the 355-nm wavelength. Again a great variability appears, sometimes for timescales as short as a few hours, and the extremes are as low as $\tau_B = 0.05$ (on 8 June, around noon) and as high as $\tau_B = 1.1$ (in the afternoon of 14 June). The optical depths measured with the two techniques follow the same diurnal evolution, confirming that good agreement exists between the two data sets. In Fig. 6 the optical depths obtained simultaneously by the

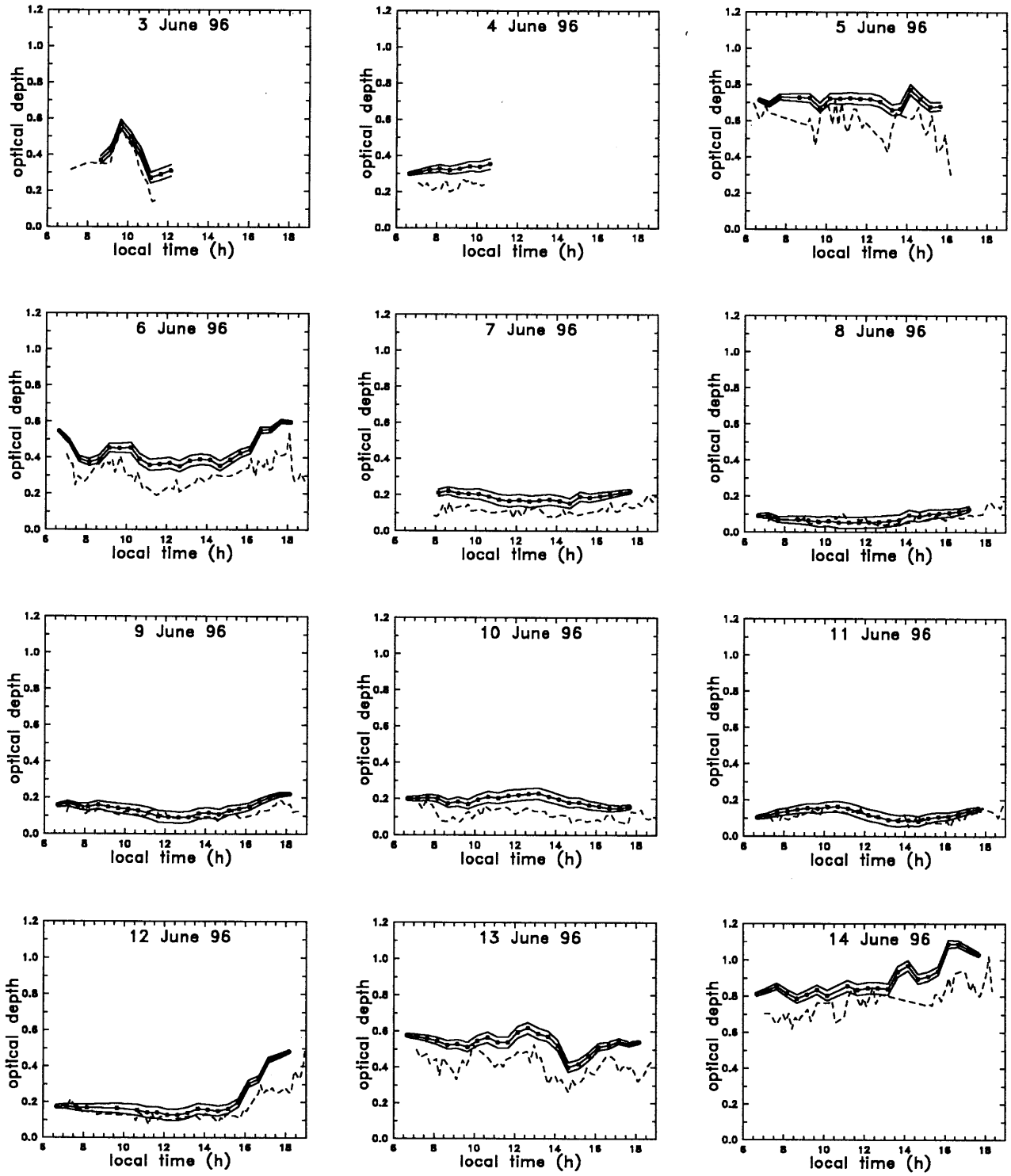

Fig. 5. Optical depths retrieved (solid curves with dots) by the Brewer spectrophotometer and (dashed curves) by lidar with the Fernald–Klett method. The other two solid curves show $\pm\Delta\tau_P$ (experimental error) of the Brewer optical depths.

Brewer instrument and by lidar are compared. The best-fit line is

$$\tau_B = a + b\tau_L \tag{16}$$

with $a = 0.041 \pm 0.004$ and $b = 1.13 \pm 0.01$. The correlation between the two methods is high (correlation coefficient 0.98). A more significant comparison can be achieved by subtraction of the contributions due to the lowest and highest layers from the data obtained with the Brewer spectrophotometer. We perform this correction empirically by assuming that the extinction coefficient is constant in the 50–600-m range and is equal to the value derived

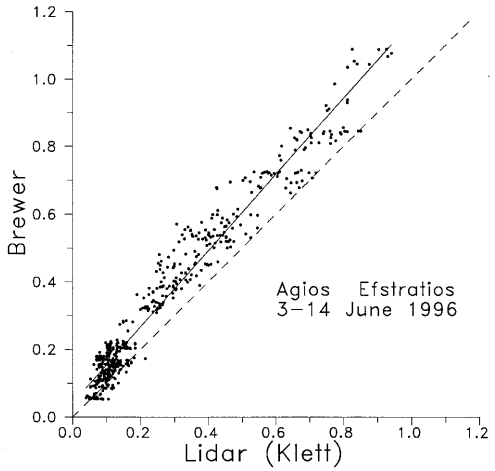

Fig. 6. Comparison of the optical depths retrieved simultaneously with the Brewer spectrophotometer in the 50-m to infinity altitude range (τ_B) and with the lidar in the 0.6–5-km altitude range (τ_L). Also shown are (solid line) a best-fit line and (dashed line) the $\tau_B = \tau_L$ line.

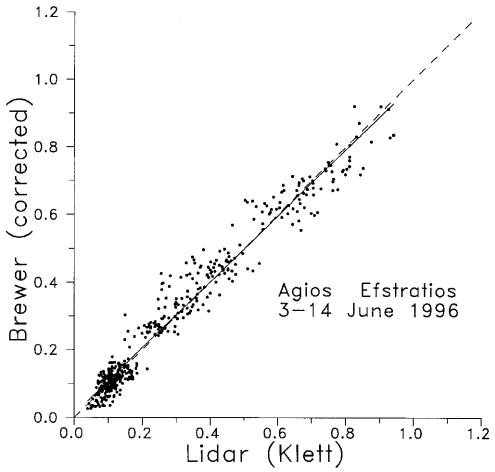

Fig. 8. Same as Fig. 6, but the optical depths measured by Brewer spectrophotometer have been corrected to remove the contribution due to the 50–600-m altitude range.

from the lidar measurement at 600 m. As for the highest layers ($z > 5$ km), their contribution has been neglected. This is possible because the aerosol layer caused by the eruption of Mount Pinatubo in 1991 has settled down; see, for instance, Fig. 7, where the stratospheric aerosol profile measured at 532 nm by lidar in Firenze, Italy (43°48′N, 11°14′E), is shown. This measurement was performed by the Istituto di Ricerca sulle Onde Elettromagnetiche—Consiglio Nationale delle Ricerche (IROE) simultaneously with the experiment on Agios Efstratios and showed that the stratospheric aerosol optical depth is smaller than 0.002 at that wavelength. The plot of the corrected Brewer optical depth, τ_B', as a function of τ_L is shown in Fig. 8. This rough correction produces a better correspondence between the two data sets. The best-fit parameters this time are $a = 0.011 \pm 0.003$ and $b = 0.976 \pm 0.009$ (correlation coefficient 0.98). The scattering of the data, visible in Fig. 8, can be attributed to the low signal-to-noise ratio of the lidar return from the largest altitudes, which makes the choice of the reference height critical, and to the roughness of the correction performed by assuming a constant α_P below 600 m. As a matter of fact the aerosol height distribution in the lowest PBL is subject to variation, even on very short timescales.

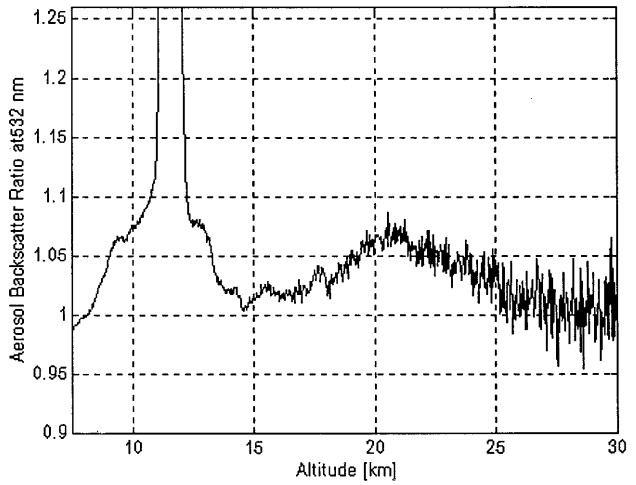

Fig. 7. Aerosol backscattering ratio, $R = (\beta_R + \beta_P)/\beta_R$, as measured at 532 nm by lidar in Firenze, Italy, on June 11, 1996. The signature of a tropospheric cloud is visible at ~12 km in height. The stratospheric aerosol layer is confined between 15 and 30 km, and its optical depth was found to be less than 0.002 at 532 nm. Courtesy of IROE.

B. Lidar and Photometric Measurements Combined

We have applied the iterative method described above by keeping the same reference height. We have chosen $\tau^* = \tau_B'$, the Brewer optical depth corrected for the lowest layers (where this correction was performed with the Fernald–Klett method). In Fig. 9 the profiles of backscattering and extinction coefficients are shown for the daily averaged lidar signal of June 13. These plots have been obtained with the iterative method and with the Fernald–Klett method. In the latter case the value of the backscatter-to-extinction ratio used was 0.05, while in the former case it was derived, and we found $C = 0.042 \pm 0.005$. The measurement error was determined (i) taking into account the error on τ^*, obtained from the uncertainty of the Brewer measurements, and assuming an additional 33% error on the contribution of the 50–600-m range, and (ii) by assuming a 5% error on β_m. We have also verified how critical the choice of the reference height is; in this case it was found to be negligible compared with the other sources of error when z_m was chosen to be in the altitude range were the lidar follows the molecular profile well (between 5 and 6 km in this case). Figure 10 shows the retrieved values of C (daily means) and the associated standard deviations. The backscatter-to-extinction ratio is more or less constant throughout the campaign and is consistent with

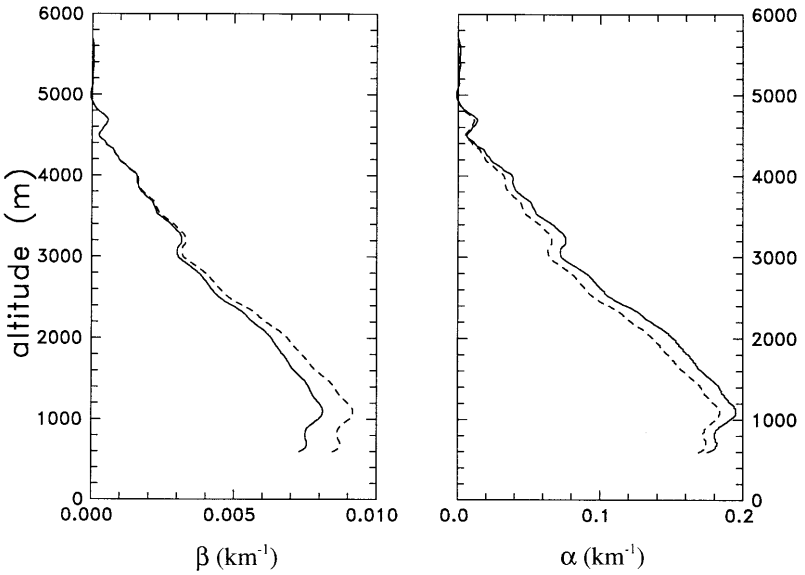

Fig. 9. Profiles of aerosol backscattering (β) and extinction (α) coefficients at 355 nm, derived with the iterative method (solid curves). Also shown is the Fernald–Klett solution (dashed curves). These curves were obtained for the daily averaged lidar profile of 13 June 1996.

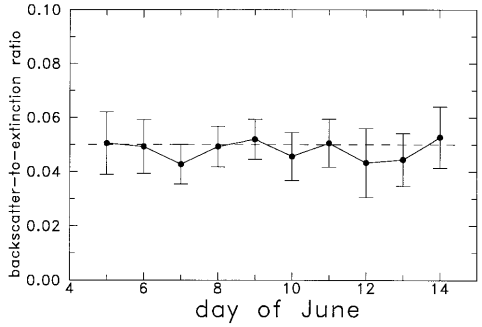

Fig. 10. Mean daily values of the backscatter-to-extinction ratio. The error bars denote the magnitude of the standard deviation. The dashed line indicates the maritime aerosol model used for an *a priori* input to the Fernald–Klett solution ($C = 0.05$).

the value assumed for a maritime aerosol model by Browell *et al.*[20]

The experiment could be improved by use of a more accurate method to perform the correction to τ_B. For instance, the Sun photometric measurements could be performed at the elevation of the lidar overlap, thus removing the necessity for a correction at the lower levels. Another possibility would be to measure independently the extinction coefficient at ground level rather than to take the value obtained with the Fernald–Klett solution at 600 m. It should also be pointed out that it is not always possible to neglect the stratospheric contribution. In a volcanic condition the method could still be used, but an independent determination of the stratospheric optical depth would be needed (for instance, by lidar).

6. Discussion and Conclusions

During the PAUR experiment, simultaneous aerosol measurements were performed at 355 nm in a summertime marine environment, by lidar and by photometric technique. The two techniques showed good agreement when the Fernald–Klett solution was applied to invert the lidar signal and a maritime value of the backscatter-to-extinction ratio C was supplied. The aerosol load was found to be highly variable in time, with values ranging between 0.05 and 1.1 for total-column optical depth during the measurement period. The high variability of the atmospheric transparency is a well-known feature; see e.g., Ref. 35. Our results show that in nonvolcanic conditions for the stratospheric aerosol layer the major contribution to the total-column particulate optical depth comes from the first 5 km of the atmosphere. The spectrophotometric measurements also allowed us to retrieve the wavelength dependence of the optical depth in the UV spectral range and to infer the Ångström coefficient m, which is an intensive property of the aerosol particles (that is, independent of quantity). The obtained values range between 1 and 4. Two regimes were found and have been correlated to the optical depth at 355 nm: For $\tau_B > 0.3$, m was found to lie between 1 and 2, while for $\tau_B < 0.2$, m was found to be near 2.5–3, and in one case the Ångström coefficient was as high as ~4.

These results can be compared with other works on the subject. Borghesi *et al.*,[36] who also performed measurements at the Mediterranean Sea, in Lecce, Italy, obtained an optical depth varying between approximately 0.3 and 4 at the same time of the year (when scaled to 355 nm with the Ångström formula). They also derived the Ångström coefficient, obtaining values between 0.5 and 1.5, with an average m of 1.1. Slightly higher values of the Ångström coefficient (as high as 1.9) were encountered by the same research team in a mountain area, at Campo Imperatore, Italy (2.2-km altitude). Although the Ångström coefficient is generally between 0.5 and 2.0 (see, e.g., Ref.

37), larger values are found in the literature. Values of $m = 2.2$ have been observed at Valladolid, Spain, for low turbidity cases,[38] and $m = 2.26$ has been found by Je and Je Tai[39] at Beijing, China. Trier and Horvath[40] show values of m as high as 3 at Santiago de Chile. Ogren and Sheridan[41] report aerosol observations carried out in the boundary layer and the free troposphere across the United States. They obtain Ångström coefficients that are always between 2 and 2.5.

For large-optical-depth conditions our results are generally in agreement with results from other groups. In the low-optical-depth regime our larger values of the Ångström coefficient generally exceed those reported in the literature. It must be mentioned, though, that the determination of the Ångström coefficient is generally made on the basis of photometric measurements in discrete bands in the visible and near infrared spectral range. The Ångström formula is an empirical fitting equation, and it is plausible that different values of the Ångström coefficient apply for different parts of the spectrum. Moreover, the determination of the Ångström coefficient with low turbidity requires the measurement of very small optical depths, possibly producing larger uncertainties in the visible and infrared, where the optical depths are smaller than in the ultraviolet. Thus it may be speculated that determinations of m in the ultraviolet spectral range are more accurate. However, it also must be noted that almost all the points on the graph in Fig. 4 are compatible with $m = 2$, within 1 standard deviation.

By using the optical parameters for the tropospheric aerosol models that are at the base of LOWTRAN, given by Selby *et al.*,[42] we have calculated the values of the Ångström coefficient in the visible (between 400 and 694 nm) and in the ultraviolet (between 300 and 400 nm). In this model the Ångström coefficient does not vary with the atmospheric turbidity. It is found between 0.23 and 1.19 in the visible and between 0.29 and 0.95 in the UV, the smallest values being for maritime aerosols. The aerosol model developed by Shettle and Fenn[43] also takes into account the effect of humidity on the optical properties of the aerosols. For relative humidity below 80% this model gives approximately the same values of m as Ref. 42, except for the maritime case (where the Ångström coefficient is higher). The Ångström coefficient from the data of Ref. 43 is calculated between 300 and 337 nm in the UV and between 337 and 694 nm in the visible. In general the Ångström coefficients derived from these models appear smaller in the UV than in the visible. They are also smaller than those obtained from our observations, but we stress that these aerosol models (in which size distribution and refractive index are given *a priori*) are quite general and probably are not able to describe correctly the different situations of the troposphere.

The large values of m obtained from the ultraviolet photometric measurement could be ascribed partly to the presence of absorbing particles. An increased absorption in the UV, as expected, for example, from organic or crustal material,[44,45] could produce a larger extinction coefficient at shorter wavelengths and thus a large Ångström coefficient. Some types of carbonaceous aerosols also show a large increase of the imaginary part of the refractive index in the UV.[46]

Results linking particle dimensions with the Ångström coefficient have been reported (see, e.g., Ref. 40), indicating that a large value of m is attributable to small aerosol particles, while a small m corresponds to large particles. Atmospheric processes leading to very low turbidity conditions are generally selective with respect to the size of the particles. This is the case, for instance, for nucleation, cloud formation, and precipitation processes and for long-range transport. In fact, aged aerosols are generally constituted by small particles, which are removed less efficiently than large ones. These processes may explain the correspondence between high turbidity and small Ångström coefficients (i.e., large particles) and between low turbidity and large values of m (small particles).

Combining the photometric and the lidar data allowed us to find an estimate of the backscatter-to-extinction ratio, which is another intensive property of the particles. In our case the value of C that was chosen *a priori* was confirmed, but in other cases the guess for this quantity can be problematic. For instance, our laboratory in Thessaloniki is situated in an urban area, but at the same time it is near the seashore, an industrial area, and rural surroundings. Different types of aerosol with different properties are expected to come from different directions, making it difficult to choose an aerosol model adequately for the selection of the backscatter-to-extinction ratio.

Our measurements of C are consistent with the value of 0.05 that is assumed for maritime aerosols by Browell *et al.*[20] Evans[22] has revised a series of 368 experimental determinations of the backscatter-to-extinction ratio obtained in the visible and at 694 nm and has performed 106 calculations of the same ratio on the basis of measurements of the aerosol size distribution. His results show that 67% of the experimental values of C fall in the range 0.05–0.06, 11% are between 0.02 and 0.04, and 22% are between 0.07 and 0.08, the last being attributed mainly to ash particles. Out of the calculated values, 82% were between 0.05 and 0.06. Our findings, although obtained in a different wavelength range, compare well with the results reported by Evans.

The backscatter-to-extinction ratios reported in Fig. 10 seem to be independent of the mean daily aerosol optical depths and Ångström coefficients, which vary considerably over the same period of time. This fact, again, must be compared with the Mie scattering calculations performed by Evans.[22] His results indicate that, for any given wavelength, specific ranges of the aerosol refractive index and size distribution exist, where C is relatively insensitive to variations of aerosol properties.

We emphasize that an experimental determination of the backscatter-to-extinction ratio could, in principle, provide more information about the particles.

Important properties such as the size distribution parameters and the refractive index could probably be deduced from Mie scattering calculations by use of simultaneously measured values of the backscatter-to-extinction ratio and the Ångström coefficient.

This research was conducted in the framework of the PAUR project, funded by the European Commission (contract ENV4-CT95-0048). F. Marenco and V. Santacesaria held a research scholarship, also awarded by the European Commission, in the framework of the Human Capital and Mobility programme (contract CHRX-CT94-0487), which is gratefully acknowledged. Thanks are extended to IROE, Firenze, for providing the stratospheric aerosol data shown in Fig. 7.

References

1. J. Reagan, J. Spinhirn, D. Byrne, D. Thomson, R. Gena, and Y. Mamane, "Atmospheric particulate properties inferred from lidar and solar radiometer observations compared with simultaneous in situ aircraft measurements: a case study," J. Appl. Meteorol. **16,** 911–928 (1977).
2. C. Brognier, R. Santer, B. Diallo, M. Herman, J. Lenoble, and H. Jaeger, "Comparative observations of stratospheric aerosols by ground-based lidar, balloon-borne polarimeter, and satellite solar occultation," J. Geophys. Res. **97,** 20,805–20,823 (1992).
3. D. Krueger, L. Caldwell, H. Alvarez, and C. She, "Self-consistent method for determining vertical profiles of aerosol and atmospheric properties using a high-spectral resolution Rayleigh–Mie lidar," J. Atmos. Oceanic Technol. **10,** 533–545 (1993).
4. H. M. Steele and P. Hamill, "Effects of temperature and humidity on the growth and optical properties of sulphuric acid-water droplets in the stratosphere," J. Aerosol Sci. **12,** 517–528 (1981).
5. D. Baumgardner, J. E. Dye, G. Barr, K. Barr, K. Kelly, and K. R. Chan, "Refractive indices of aerosols in the upper troposphere and lower stratosphere," Geophys. Res. Lett. **23,** 749–752 (1996).
6. P. B. Russell, T. J. Swissler, and M. P. McCormick, "Methodology for error analysis and simulation of lidar aerosol measurements," Appl. Opt. **18,** 3783–3797 (1979).
7. Y. Sasano, E. V. Browell, and S. Ismail, "Error caused by using a constant extinction/backscattering ratio in the lidar solution," Appl. Opt. **24,** 3929–3932 (1985).
8. P. Di Girolamo, M. Cacciani, A. Di Sarra, G. Fiocco, and D. Fuà, "Lidar observations of the Pinatubo aerosol layer at Thule, Greenland," Geophys. Res. Lett. **21,** 1295–1298 (1994).
9. G. F. Fernald, "Analysis of atmospheric lidar observations: some comments," Appl. Opt. **23,** 652–653 (1984).
10. J. D. Klett, "Lidar inversion with variable backscatter/extinction ratios," Appl. Opt. **24,** 1638–1643 (1985).
11. R. M. Endlich, F. L. Ludwig, and E. E. Uthe, "An automated method for determining the mixing depth from lidar observations," Atmos. Environ. **13,** 1051–1056 (1979).
12. S. H. Melfi, J. D. Spinhirne, S.-H. Chou, and S. P. Palm, "Lidar observations of vertically organised convection in the Planetary Boundary Layer," J. Clim. Appl. Meteorol. **24,** 806–821 (1985).
13. T. D. Crum, R. B. Stull, and E. W. Eloranta, "Coincident lidar and aircraft observations of entrainment into thermals and mixed layers," J. Clim. Appl. Meteorol. **26,** 774–788 (1987).
14. D. I. Cooper and W. E. Eichinger, "Structure of the atmosphere in an urban planetary boundary layer from lidar and radiosonde observations," J. Geophys. Res. **99,** 22,937–22,948 (1994).
15. T. Takamura, Y. Sasano, and T. Hayasaka, "Tropospheric aerosol optical properties derived from lidar, sun photometer, and optical particle counter measurements," Appl. Opt. **33,** 7132–7140 (1994).
16. A. Papayannis, D. Balis, A. Bais, H. van der Bergh, B. Calpini, E. Durieux, L. Fiorani, L. Jacquet, I. Ziomas, and C. S. Zerefos, "The role of urban and suburban aerosols on solar UV radiation over Athens, Greece," Urban Environ. (to be published).
17. D. S. Balis, A. F. Bais, A. Papayannis, F. Marenco, V. Santacesaria, and C. S. Zerefos, "Comparison of model calculations with spectral solar UV measurements," in *Proceedings of the XVIII Quadriennal Ozone Symposium*, G. Visconti and R. Bojkov, eds. (Parco Scientifico e Tecnologico d'Abruzzo, to be published).
18. R. T. H. Collis and P. B. Russell, "Lidar measurements of particles and gases by elastic backscattering and differential absorption," in *Laser Monitoring of the Atmosphere*, E. D. Hinkley, ed. (Springer-Verlag, Berlin, 1976), pp. 71–151.
19. U.S. Standard Atmosphere (National Oceanic and Atmospheric Administration, NASA, U.S. Air Force, Washington, D. C., October 1976).
20. E. V. Browell, S. Ismail, and S. T. Shipley, "Ultraviolet DIAL measurements of O_3 profiles in regions of spatially inhomogeneous aerosols," Appl. Opt. **24,** 2827–2836 (1985).
21. T. Takamura and Y. Sasano, "Ratio of aerosol backscatter to extinction coefficients as determined from angular scattering measurements for use in atmospheric lidar applications," Opt. Quantum Electron. **19,** 293–302 (1987).
22. B. T. N. Evans, "Sensitivity of the backscatter/extinction ratio to changes in aerosol properties: implications for lidar," Appl. Opt. **27,** 3299–3306 (1988).
23. V. A. Kovalev, "Sensitivity of the lidar solution to errors of the aerosol backscatter-to-extinction ratio: influence of a monotonic change in the aerosol extinction coefficient," Appl. Opt. **34,** 3457–3462 (1995).
24. V. A. Kovalev, "Lidar measurements of the vertical aerosol extinction profiles with range-dependent backscatter-to-extinction ratios," Appl. Opt. **32,** 6053–6065 (1993).
25. A. Papayannis and D. Balis, "Study of the structure of the lower troposphere over Athens using a backscattering lidar during the MEDCAPHOT-TRACE experiment: measurements over a suburban area," Urban Environ. (to be published).
26. T. Halldorsson and J. Langerholc, "Geometrical form factors for the LIDAR function," Appl. Opt. **17,** 240–244 (1978).
27. A. F. Bais, C. S. Zerefos, and C. T. McElroy, "Solar UVB measurements with the double- and single-monochromator Brewer ozone spectrophotometer," Geophys. Res. Lett. **23,** 833–836 (1996).
28. A. F. Bais, "Absolute spectral measurements of the direct solar ultraviolet irradiance using a Brewer spectrophotometer," Appl. Opt. **36,** 5199–5204 (1997).
29. M. E. Vanhoosier, J. F. Bartoe, G. E. Brueckner, and D. K. Prinz, "Absolute solar spectral irradiance 120nm-400nm (results from the Solar Ultraviolet Spectral Irradiance Monitor-SUSIM-experiment on board Spacelab-2)," Astron. Lett. Commun. **27,** 163–168 (1988).
30. J. E. Hansen and L. D. Travis, "Light scattering in planetary atmospheres," Space Sci. Rev. **16,** 527 (1974), as reported by H. R. Gordon, J. W. Brown, and R. H. Evans, "Exact Rayleigh scattering calculations for use with the Nimbus-7 coastal zone color scanner," Appl. Opt. **27,** 862–871 (1988).
31. P. M. Teillet, "Rayleigh optical depth comparisons from various sources," Appl. Opt. **29,** 1897–1900 (1990).
32. L. T. Molina and M. J. Molina, "Absolute cross sections of ozone in the 185- to 350-nm wavelength range," J. Geophys. Res. **91,** 14,501–14,508 (1986).
33. M. Cacciani, A. di Sarra, G. Fiocco, and A. Amoruso, "Absolute determination of ozone in the wavelength region 339-355 nm

at temperatures 220-293 K," J. Geophys. Res. **94,** 8485–8490 (1989).
34. A. Angstrom, "On the atmospheric transmission of sun radiation and on dust in the air," Georg. Ann. Deutch. **12,** 156 (1929), as reported by E. Trakhovsky and E. P. Shettle, "Wavelength scaling of atmospheric aerosol scattering and extinction," Appl. Opt. **26,** 5148–5153 (1987).
35. K. Y. Kondratyev, *Radiation in the Atmosphere* (Academic, New York, 1969).
36. A. Borghesi, E. Bussoletti, G. Falcicchia, and A. Minafra, "Determination of atmospheric water vapour and turbidity parameters from diurnal infrared hygrometer and turbidimeter data," Infrared Phys. **22,** 149–155 (1982).
37. D. P. Woodman, "Limitations in using atmospheric models for laser transmission estimates," Appl. Opt. **13,** 2193–2195 (1974).
38. V. E. Cachorro and J. L. Casanova, "Punctualizaciones sobre diversos aspectos en la utilizacion de la formula de Angstrom," Rev. Geofis. **45,** 123–130 (1989), as reported in Ref. 40.
39. L. Je and M. Je Tai, "Properties of the atmospheric aerosols inverted from optical remote sensing," Atmos. Environ. Part A **24,** 2512–2522 (1990).
40. A. Trier and H. Horvath, "A study of the aerosol of Santiago de Chile. II: mass extinction coefficients, visibilities and Angstrom exponents," Atmos. Environ. Part A **27,** 385–395 (1993).
41. J. A. Ogren and P. J. Sheridan, "Vertical and horizontal variability of aerosol single scattering albedo and hemispheric backscatter fraction over the United States" in *Nucleation and Atmospheric Aerosols 1996*, M. Kulmala and P. E. Wagner, eds. (Elsevier, New York, 1996), pp. 780–783.
42. J. E. A. Selby, E. P. Shettle, and R. A. McClatchey, "Atmospheric transmittance from 0.25 to 28.5 micron: supplement to LOWTRAN 3B (1976)," Rep. AFGL-TR-76-0258 U.S. Air Force Geophysics Laboratory, Hanscom Air Force Base, Mass., 1976).
43. E. P. Shettle and R. W. Fenn, "Models for the aerosols of the lower atmosphere and the effects of humidity variations on their optical properties," Rep. AFGL-TR-79-0214, Air Force Geophysics Laboratory, Hanscom Air Force Base, Mass., 1979).
44. Y. S. Lyubotseva and L. G. Yaskovich, "Aerosol absorption within the wavelength interval 0.25 to 0.8 micron," Izv. Akad. Nauk SSSR Ser. Fiz. Atmos. Okeana **18,** 922–932 (1982), as reported by H. Horvath, "Atmospheric light absorption-a review," Atmos. Environ. Part A **27,** 293–317 (1993).
45. E. M. Patterson, "Optical properties of the crustal aerosol: relation to chemical and physical characteristics," J. Geophys. Res. **86,** 3236–3246 (1981).
46. J. T. Twitty and J. A. Weinman, "Radiative properties of carbonaceous aerosols," J. Appl. Meteorol. **10,** 725–731 (1971).